processes

MDPI

Article

An Exploratory Approach to Sustainable Esterase Production Through Co-Valorization of Cheese Whey and Vegetable Wax for Supported Solid-State Fermentation by *Serratia marcescens* 11E

Francisco Javier Aranda-Valdés [1,2], Iris Cristina Arvizu-De León [1,2], Gabriela Elizabeth Quintanilla-Villanueva [1,2], Edgar Allan Blanco-Gámez [1,2], Juan Francisco Villarreal-Chiu [1,2,*] and Melissa Marlene Rodríguez-Delgado [1,2,*]

[1] Universidad Autónoma de Nuevo León, Facultad de Ciencias Químicas, Av. Universidad S/N Ciudad Universitaria, San Nicolás de los Garza 66455, Mexico; francisco.arandav@uanl.edu.mx (F.J.A.-V.); iris.arvizudl@uanl.edu.mx (I.C.A.-D.L.); gquintanillav@uanl.edu.mx (G.E.Q.-V.); edgar.blancogmz@uanl.edu.mx (E.A.B.-G.)

[2] Centro de Investigación en Biotecnología y Nanotecnología (CIByN), Facultad de Ciencias Químicas, Universidad Autónoma de Nuevo León, Parque de Investigación e Innovación Tecnológica, Km. 10 Autopista al Aeropuerto Internacional Mariano Escobedo, Apodaca 66629, Mexico

* Correspondence: juan.villarrealch@uanl.edu.mx (J.F.V.-C.); melissa.rodriguezdl@uanl.edu.mx (M.M.R.-D.)

Abstract

Lipolytic and esterase-like enzymes are crucial in the food industry for flavor production and ester hydrolysis. This study presents an exploratory, baseline feasibility approach to evaluate esterase-like enzyme production by *Serratia marcescens* 11E via a sustainable co-valorization matrix, where vegetable wax residues serve as structural solid support and cheese whey acts as the primary lipid nutritional source. Under fixed 48-h screening conditions, the recovered cell-free extract exhibited a distinct catalytic preference for short-chain esters, showing higher specific activity toward 4-nitrophenyl acetate (0.743 U/mg) than 4-nitrophenyl palmitate (0.125 U/mg), confirming a predominant carboxylesterase-like profile. Biochemical characterization revealed an initial optimal activity at pH 9.0 and 30 °C, along with a noteworthy bimodal catalytic behavior featuring a secondary activity peak at 70 °C. Size-exclusion chromatography resolved the extract into two distinct active elution pools (17.8 and 26.2 U/mg), which corresponded to candidate protein bands of 35–40 kDa on SDS-PAGE. Although definitive molecular identification remains subject to ongoing zymographic and proteomic characterization, these foundational findings demonstrate the potential of co-valorizing lipid- and carbohydrate-rich industrial wastes to produce resilient proteins with esterase-like activity at elevated temperatures.

Keywords: enzymes; esterase; valorization; *Serratia marcescens*; solid-state fermentation

Academic Editors: Carlos Gregorio Barreras-Urbina, Tomás J. Madera-Santana and Betzabe Ebenhezer Lopez-Corona

Received: 9 May 2026
Revised: 16 June 2026
Accepted: 22 June 2026
Published: 26 June 2026

1. Introduction

The ongoing increase in the global population has led to a significant rise in the demand for goods, services, and natural resources, especially food and water. While this has fueled industrial and agricultural growth, it has also led to a concerning surge in waste production [1]. Inadequate management of these wastes poses a major environmental risk, underscoring the urgent need for sustainable waste-utilization solutions. The valorization of agricultural and industrial residues plays a crucial role in the circular economy by reducing environmental impact through transforming waste into valuable resources [2].

Approximately 68% of global municipal waste remains unutilized, representing a missed opportunity to recover resources, alleviate ecosystem stress, and reduce disposal costs [1].

Nutrient-rich wastes, such as used oil cakes, fruit peels, wheat bran, bagasse, and food and dairy by-products, are highly suitable substrates for biotechnological applications, including microbial fermentation [3–6]. These processes can yield valuable products like pigments, bioplastics, biofuels, and enzymes [7–10]. In particular, enzyme production is highly relevant to industry, especially for the α/β hydrolase fold family, including esterases and lipases, due to their ability to catalyze a wide range of reactions, including hydrolysis, esterification, transesterification, and amidation [11,12]. These enzymes exhibit remarkable stability over a wide temperature and pH range, demonstrating high versatility for use across multiple sectors, including food processing [11]. In this sense, lipases are essential in industries such as dairy, baking, and alcohol production, despite representing less than 10% of the global enzyme market [13]. They play a key role in developing the characteristic flavors of cheese, butter, and margarine via fat hydrolysis. In addition to flavor development, lipases influence wine aroma profiles and help preserve the freshness of baked goods [14]. Esterases are equally important in the food and beverage sector, used to refine oils and fats, process fruit juices, and synthesize specific scents and flavors. In the dairy industry, they are essential for cheese making, aiding the formation of methyl and ethyl esters from short-chain fatty acids, which contribute distinct fruity flavor notes [15].

Despite their structural similarities, lipases and esterases are distinguished by their substrate specificity: esterases preferentially hydrolyze short-chain triglycerides and water-soluble substrates, whereas true lipases act on long-chain, water-insoluble triglycerides at an oil–water interface [4,16]. Traditionally, these hydrolases have been produced through submerged fermentation (SmF) using microorganisms such as *Pseudomonas aeruginosa*, *Micrococcus roseus*, *Serratia marcescens*, and *Saitozyma flava* [17–20]. Although SmF is well established, it presents notable drawbacks, including the generation of large volumes of effluent and high operational costs [21]. Consequently, solid-state fermentation (SSF) has gained significant attention due to its operational and economic advantages, including lower energy requirements, improved metabolite yields, and the feasibility of using raw agro-industrial residues directly as solid matrices [21,22].

Through SSF, practical production thresholds have been achieved by utilizing agro-industrial wastes as substrates. For instance, studies have reported yields of 826 U/gds from *Rhizopus homotallicus* grown on sugarcane bagasse [6], 6.66 U/gds from *Micrococcus roseus* under low-temperature conditions [20], and up to 107.44 U/gds from *Pseudomonas* sp. BUP6 on oily residues [23]. Additionally, success has been reported in non-sterile environments and using microbial consortia [24,25]. Different classes of esterases have demonstrated immense potential in bioprocesses. For instance, carbohydrate esterases are used in the treatment of lignocellulosic feedstock [26] and for biofuel production [27], while esterases from *Bacillus* species can process olive oil to synthesize biosurfactants [28,29]. Therefore, exploring low-cost production alternatives for enzymes with high industrial applicability remains a growing area of interest. In this context, assessing wild-type microbial strains capable of utilizing complex regional residues as an alternative culture is essential.

The present study aims to investigate the production of esterases by *Serratia marcescens* 11E via SSF, using an exploratory, baseline feasibility approach. Within this framework, a sustainable co-valorization matrix is established in which industrial residues from vegetable wax serve as a solid structural support, and cheese whey acts as the primary liquid nutrient and moisture vehicle. Under fixed operational screening conditions, the recovered cell-free extract was biochemically characterized to evaluate its preliminary catalytic performance over a range of temperatures, pH values, and substrate acyl chain lengths. This work seeks to establish a foundational proof-of-concept for revalorizing lipid- and carbohydrate-rich

industrial wastes into resilient, candidate protein streams exhibiting esterase-like activity for potential applications in the food industry.

2. Materials and Methods

2.1. Microorganisms and Chemicals

The wild-type *Serratia marcescens* 11E strain was originally isolated from Bustamante National Park in Nuevo León, Mexico [30]. The culture was stored in Luria–Bertani (LB) broth containing 20% (*v*/*v*) glycerol at −20 °C. Reactivation was performed in LB broth and incubated at 24 °C and 150 rpm for 24 h on a rotary shaker (SHELL-LAB 1574 incubator, Sheldon Manufacturing, Inc., Cornelius, OR, USA). Culture media, including LB broth and LB agar, were obtained from BD Biosciences (San Jose, CA, USA). Reagents such as phosphate-buffered saline (PBS), p-nitrophenyl acetate (pNPA), p-nitrophenyl butyrate (pNPB), p-nitrophenyl octanoate (pNPO), p-nitrophenyl palmitate (pNPP), bovine serum albumin (BSA), and Tris-HCl buffer components were purchased from Sigma-Aldrich (St. Louis, MO, USA). The molecular weight marker (Invitrogen™ SeeBlue™ Pre-stained Protein Standard, 3–198 kDa) for SDS-PAGE analysis was purchased from Fisher-Scientific (Waltham, MA, USA).

2.2. Qualitative Screening and Culture Purity Validation

A preliminary qualitative assay was performed to verify the lipolytic and esterase-like screening profiles of *Serratia marcescens* 11E and to serve as an additional internal quality control checkpoint to confirm baseline culture purity. The culture was streaked onto tributyrin agar (20 g/L) supplemented with calcium chloride dihydrate ($CaCl_2 \cdot 2H_2O$, 0.1 g/L) and Tween 80 (10 mL/L) as a selective sorbitol ester containing an 18-carbon fatty acid chain. The plates were incubated at 30 °C for 48 h under aerobic conditions. Lipolytic activity was identified by the development of a distinct white, opaque halo of precipitation around the colonies, resulting from localized hydrolysis of the substrate and subsequent precipitation of insoluble calcium fatty acid salts. The macro- and microscopic morphologies confirming strain authenticity and purity during this baseline validation phase are provided in the Supporting Information (Figure S1).

2.3. Supported Production Media and Culture Conditions

Enzyme production was conducted via supported solid-state fermentation (SSF) using an 80:20 (*w*/*w*) co-valorization matrix composed of agro-industrial and dairy residues. In this operational configuration, industrial vegetable wax candle residues served as a hydrophobic, structural solid support, while crude cheese whey sourced from a local dairy acted as the liquid nutritional vehicle and moisture phase. Both raw substrates were thoroughly characterized: the fatty acid profile of the wax was analyzed according to the AOAC 969.33 saponification and transesterification method [31]. The cheese whey was characterized for moisture content (%) in accordance with the NOM-116-SSA1-1994 standard [32], while total sugars and total carbohydrates (%) were quantified following the protocols established in NOM-086-SSA1-1994 [33].

The bioprocess was conducted using 50 g of the prepared solid-state wax/cheese whey medium, adjusted to an initial pH of 9.0 and incubated at 37 °C for 48 h. An overnight culture of *S. marcescens* 11E grown in LB broth (30 °C, 24 h, 150 rpm) was used as the inoculum to seed the matrix at 1% (*v*/*v*), achieving an initial cell density of OD_{600} = 0.1. Following the 48-h fermentation period, the extracellular enzyme fraction was recovered by clarification via centrifugation at 9000 rpm and 4 °C for 15 min. The resulting cell-free supernatant, designated as the crude extract, was gently concentrated

under non-denaturing native conditions via ultrafiltration using a 50-kDa molecular weight cut-off (MWCO) polyethersulfone membrane prior to biochemical analysis.

2.4. Enzyme and Protein Assays

Esterase-like catalytic activity was monitored spectrophotometrically using a Cary 50 spectrophotometer (Varian Inc., Palo Alto, CA, USA) by tracking the rate of absorbance increase at 410 nm released via the cleavage of p-nitrophenyl acetate (pNPA). The standard reaction mixture (1.0 mL total volume) consisted of 500 µL of 0.15 M phosphate buffer (pH 7.4), 0.5% Triton X-100 as surfactant stabilizer, 20 µL of pNPA dissolved in acetonitrile, and 30 µL of the crude enzyme extract. This mixture was pre-warmed and incubated at 30 °C for 15 min. The reaction was immediately terminated and alkalinized by adding 500 µL of 0.5 M Tris-HCl buffer (pH 9) to maximize the molar absorptivity of the released p-nitrophenol anion. One international unit of enzymatic activity (U) was defined as the amount of enzyme exhibiting esterase-like traits that releases 1 µmol of p-nitrophenol per minute under the designated assay conditions [34].

Total protein concentration was quantified by the Bradford method [35], utilizing bovine serum albumin as the calibration standard. Specific activity (U/mg) was systematically calculated as the ratio of total catalytic units to the total protein mass (mg) present in the sample.

2.5. Characterization of Crude Extract: Impact of Temperature, pH, and Substrate Affinity

To map the operational boundaries and possible bimodal profiles of the recovered extract, enzymatic activity was systematically screened over a temperature range of 30–70 °C (with a fixed 15-min reaction window) and a pH range of 5.0–11.0. The pH thresholds were rigorously adjusted directly at the targeted reaction temperatures using 0.15 M buffer matrices: sodium acetate-citrate buffer for pH 5.0–6.0, Tris-HCl buffer for pH 7.0–9.0, and sodium carbonate buffer for pH 10.0–11.0. The independent impacts of pH and temperature effects were quantified spectrophotometrically at 410 nm using 0.05 M pNPA as the substrate under the reaction architecture described in Section 2.4.

To further elucidate the biocatalytic profile of the extract and determine whether the active fractions possessed a distinct carboxylesterase or true lipase bias, substrate specificity assays were conducted under standard reaction boundaries using a panel of p-nitrophenyl esters with varying fatty acids of varying chain lengths: p-nitrophenyl butyrate (pNPB, C4), p-nitrophenyl octanoate (pNPO, C8), and p-nitrophenyl palmitate (pNPP, C16), alongside the baseline pNPA (C2) assay. Substrate preference was interpreted based on relative hydrolytic efficiency toward water-soluble short-chain versus water-insoluble long-chain configurations.

2.6. Streamlined Downstream Fractionation and Protein-Profile Analysis

To preserve the enzyme mass balance in the small-scale SSF matrix and to eliminate low-molecular-weight agro-industrial interferences, a streamlined, preparative downstream strategy was developed. The crude concentrate was loaded onto a size-exclusion chromatography column packed with Sephadex G-100 (Merck KGaA, Darmstadt, Germany) (stationary phase), allowed to settle, and equilibrated overnight. Washing was performed with one column volume of distilled water at a constant operational flow rate of 0.5 mL/min. Elution and functional fractionation were carried out using two columns, with 0.15 M Tris–HCl buffer (pH 8.5) as the mobile phase. Absorbance at 280 nm was evaluated at the column exit strictly as a qualitative, real-time screening threshold for detecting protein elution boundaries and guiding sample collection.

The individual collected fractions were systematically assayed for esterase-like activity. The fractions with the highest specific activities were pooled into discrete active

elution pools and concentrated via native ultrafiltration using a 50-kDa MWCO membrane. A quantitative enzyme purification table was compiled to monitor total volume, total protein, total activity, specific activity, yield recovery, and purification fold across the streamlined pipeline.

The denatured monomeric molecular mass profiles of the enriched candidate fractions were evaluated by sodium dodecyl sulfate–polyacrylamide gel electrophoresis (SDS-PAGE) according to the Laemmli method [36]. Electrophoresis was performed using 12% acrylamide resolving gels, stained with Coomassie Brilliant Blue R250, and visualized with the Invitrogen™ SeeBlue™ Pre-stained Protein Standard (3–198 kDa; Fisher-Scientific, Waltham, MA, USA) as the molecular weight marker.

2.7. Statistical Analysis

All solid-state fermentation runs and subsequent biochemical characterization assays were performed in independent triplicate (n = 3). A clear distinction was maintained between biological replicates (three entirely parallel SSD culture batches to capture operational and matrix variability) and technical replicates (triplicate parallel instrumental readings of each individual biological sample to minimize micro-pipetting errors). Quantitative data gathered across this study are strictly expressed and reported as the experimental mean ± standard deviation (±SD).

3. Results

The qualitative screening on tributyrin agar supplemented with Tween 80 confirmed that *Serratia marcescens* 11E secreted active extracellular hydrolases capable of breaking ester bonds. After 48 h of incubation at 30 °C, the colonies developed broad, opaque white halos around the growth zone (Figure 1). This phenomenon indicates active, localized hydrolysis of the emulsified substrate and subsequent precipitation of insoluble calcium fatty acid salts. This robust hydrolytic phenotype confirmed that the wild-type strain produces extracellular biocatalysts capable of degrading ester bonds in short- and medium-chain lipid domains, thereby establishing its potential for downstream bioprocess applications. Concurrently, basic phenotypic verification regarding culture purity and macro/microscopic morphology was cross-referenced and validated (Supplementary Figure S1).

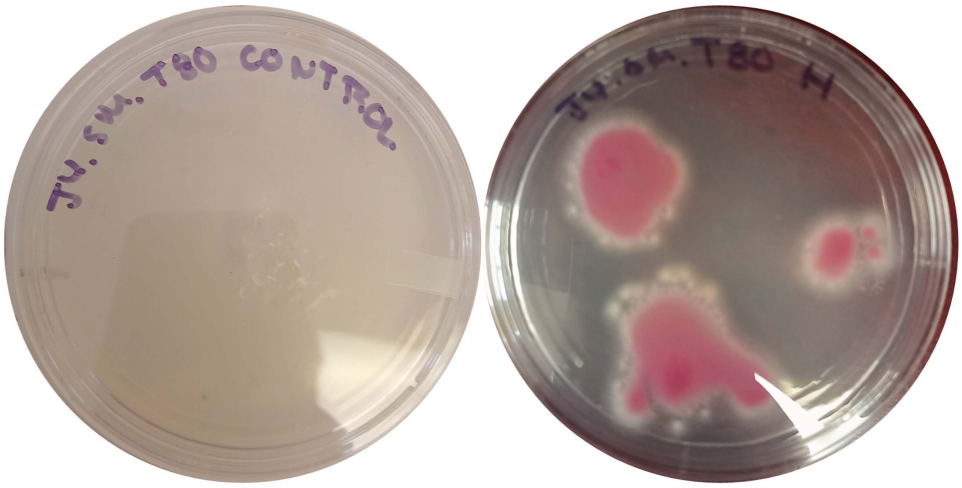

Figure 1. Qualitative screening of the biocatalytic capacity of *Serratia marcescens* 11E on tributyrin agar supplemented with Tween 80 after 48 h of incubation at 30 °C. The uninoculated control plate (**left**) displays a homogeneous, emulsified matrix, whereas the inoculated plate (**right**) exhibits distinct white, opaque precipitation halos surrounding the colonies, confirming localized esterase-like substrate hydrolysis and the subsequent formation of insoluble calcium fatty acid salts.

The culture medium for esterase-like enzyme production via supported SSF was structured using an 80:20 (*w*/*w*) ratio of regional industrial residues. The empirical physicochemical characterization of the liquid cheese whey substrate is detailed in Table 1, which shows a high moisture content (93.86 ± 0.12%), moderate carbohydrate levels (4.20 ± 0.05%), and a low baseline protein content (0.20 ± 0.01%), consistent with typical regional dairy effluents.

Table 1. Physicochemical and proximal composition characterization of the raw cheese whey effluent used as the liquid nutritional vehicle for supported solid-state fermentation.

Parameter	Content (%)
Moisture	93.86
Total sugars	3.78
Total Carbohydrates	4.20
Protein	0.20
Fat	1.22
Ash	0.52
NaCl	0.23
pH	6.0

Meanwhile, the solid vegetable wax portion used as the hydrophobic structural support was highly enriched in saturated fatty acids (70.32%), featuring major structural components such as margaric acid (C17:0), stearic acid (C18:0), and arachidonic acid (C20:4), along with notable polyunsaturated fatty acids (29.68%) (please refer to Table 2). This balanced combination of hydrophobic and hydrophilic matrices provided a balanced carbon source, enabling *S. marcescens* 11E to establish growth while secreting targeted hydrolases under fixed operational boundaries.

Table 2. Composition and fatty acid profile of the regional industrial vegetable wax residue utilized as the hydrophobic structural support for supported solid-state fermentation.

Parameter	Content (%)
Saturated fatty acids	70.32
Monounsaturated fatty acids	<0.1
Polyunsaturated fatty acids	29.68
Pentadecanoic acid (C15:0)	4.50
Palmitic acid (C16:0)	7.14
Margaric acid (C17:0)	14.0
Stearic acid (C18:0)	13.56
Linoleic acid (C18:2)	11.69
Arachidonic acid (C20:4)	15.24
Eicosadienoic acid (C20:2)	10.49
Behenic acid (C22:0)	6.94
Docosadienoic acid (C22:2)	7.50
Lignoceric acid (C24:0)	8.94

The cell-free crude extract recovered after the 48-h SSF cycle, and the active fractions were pooled, concentrated, and adjusted to a standardized final volume of 10 mL before determination of protein concentration and enzymatic activity. The extract exhibited an average total protein concentration of 0.394 mg/mL. Initial substrate specificity using a panel of p-nitrophenyl esters demonstrated a distinct catalytic preference for short-chain fatty acids. The highest specific activity was observed for p-nitrophenyl acetate (pNPA, C2), achieving a maximum of 0.743 ± 0.03 U/mg. As the acyl chain length of the substrate increased, a significant and progressive reduction in catalytic activity was recorded. Hydrolysis dropped to 0.399 ± 0.02 U/mg for p-nitrophenyl butyrate (pNPB,

C4) and decreased further to a baseline value of 0.125 ± 0.01 U/mg when challenged with p-nitrophenyl octanoate (pNPO, C8). Finally, negligible or background activity was detected against the long-chain substrate p-nitrophenyl palmitate (pNPP, C16). This marked catalytic hierarchy (pNPA > pNPB > pNPO >> pNPP) strongly points toward a predominant carboxylesterase-like profile rather than a true lipase mechanism, which typically exhibits a thermodynamic bias toward long-chain, water-insoluble triglycerides.

Biochemical screening revealed that the crude extract maintained operational catalytic activity across a wide experimental architecture, spanning temperatures from 30 to 70 °C and pH values from 7.0 to 11.0 (Figure 2). The system exhibited optimal performance initially at 30 °C and pH 9.0, followed by a gradual thermal inactivation profile as temperatures exceeded 50 °C under neutral-to-alkaline conditions. Notably, a distinct secondary activity was consistently resolved at 70 °C and pH 9.0. This catalytic behavior could arise from localized shifts in substrate-solvent solubility matrices or thermal variations in buffer ionization constants, resulting in a robust operating profile. This behavior can be considered bimodal, as it exhibits two clearly differentiated peaks of activity at different temperatures. Compared with literature benchmarks, this candidate extract exhibits promising traits for moderate-to-high-temperature bioprocesses. For instance, Jiang et al. cloned an esterase-encoding gene (estS, 909 bp) from *Serratia* sp. in *Escherichia coli* DE3 (BL21), obtaining a recombinant enzyme with thermal limits capped at 50 °C [37], while Bhardwaj et al. isolated an esterase from *Serratia* sp. exhibiting a half-life of 3 h at 60 °C [38].

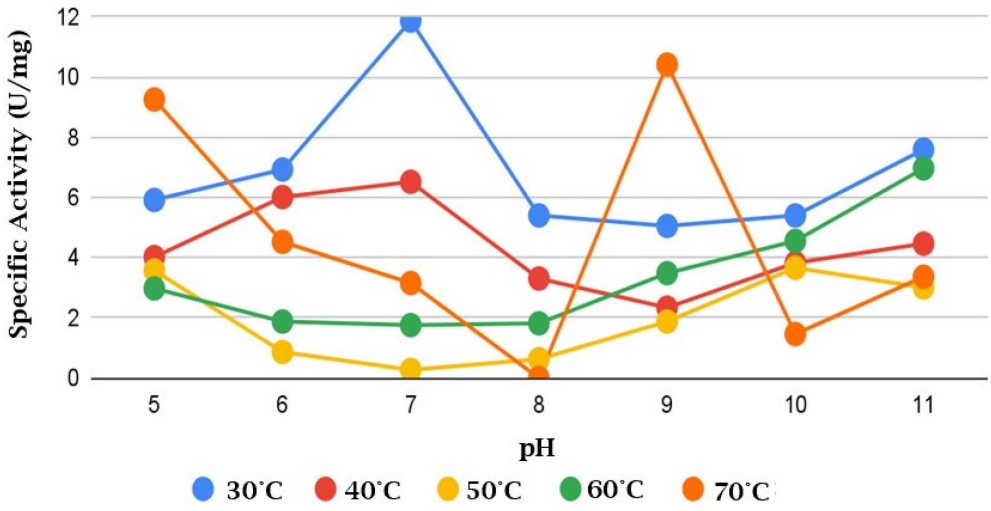

Figure 2. Multifactorial biochemical characterization of the *Serratia marcescens* 11E crude cell-free extract, mapping the operational boundaries of esterase-like catalytic activity. The evaluation illustrates relative hydrolytic velocities across an experimental architecture spanning 30–70 °C and 5.0–11.0 pH, using pNPA as the substrate.

To complement these functional findings, denaturing electrophoresis (SDS-PAGE) was used to map the protein profile of the active streams (Figure 3). Visually calibrated against the prestained standard (Lane 1) and a commercial *Pseudomonas fluorescens* lipase control (Lane 2; resolving major bands at ~41 and ~10 kDa), the crude cell-free extract from *S. marcescens* 11E (Lane 3) resolved a prominent candidate band migrating at approximately 40 kDa, alongside a fainter secondary band near 30 kDa. This molecular profile falls strictly within the structural monomeric mass ranges documented for wild-type microbial enzymes in the α/β hydrolase fold family.

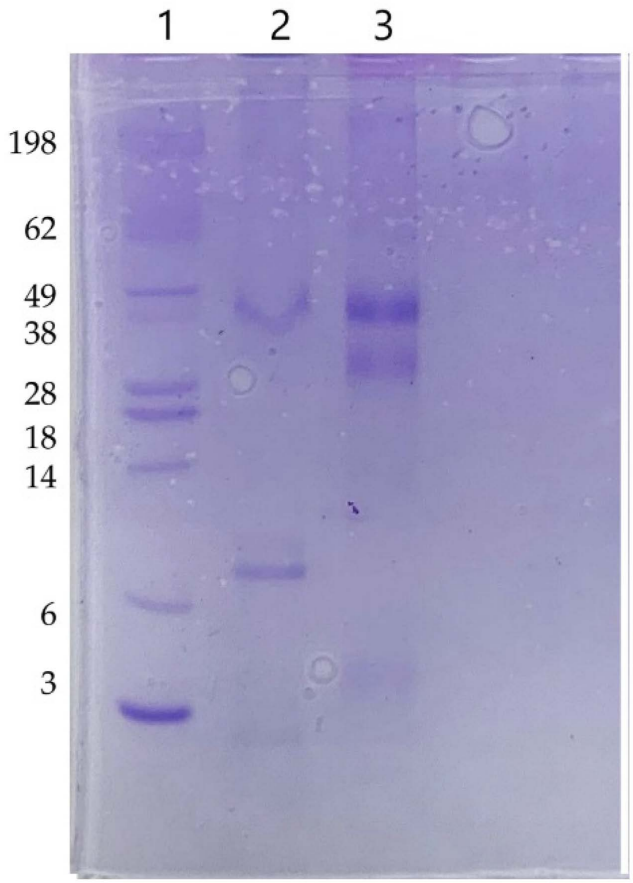

Figure 3. Denaturing sodium dodecyl sulfate–polyacrylamide gel electrophoresis (12% SDS-PAGE) profiling to monitor protein clearance and structural candidate fractions of the cell-free streams. Lane 1: Invitrogen™ SeeBlue™ Pre-stained Protein Standard (3–198 kDa); Lane 2: Commercial *Pseudomonas fluorescens* lipase control (resolving distinct bands at ~41 kDa and ~10 kDa); Lane 3: Crude cell-free extract from *Serratia marcescens* 11E, resolving a prominent candidate protein band migrating at approximately 40 kDa, visually compatible with microbial carboxylesterases.

To reinforce these electrophoretic observations and circumvent current limitations in direct protein sequencing, an in silico proteomic screening of annotated *Serratia* assemblies hosted in the National Center for Biotechnology Information (NCBI) Protein Reference Sequences database was conducted. Utilizing the representative carboxylesterase/lipase family protein sequence (WP_286093549.1) as a query blueprint, a comparative analysis across wild-type *Serratia* proteomes revealed a highly conserved, genus-wide repertoire of lipolytic proteins. This distribution exhibits a clear predominance of sequences encoding carboxylesterases (EC 3.1.1.1) over classical long-chain lipases (EC 3.1.1.3), with this predominance prominent across *S. marcescens*, *S. ureilytica*, *S. surfactantfaciens*, and *S. liquefaciens*. Crucially, the alignment demonstrated that most homologs have a polypeptide length of 511–533 amino acids, including the well-characterized carboxylesterase type B architecture, which consistently yields theoretical molecular masses of 34.5–42.1 kDa. Furthermore, established biochemical benchmarks for these family-specific enzymes confirm a solvent-accessible active-site configuration that exhibits an evolutionary thermodynamic preference for short-chain fatty acid esters (<C4) and displays negligible turnover rates when challenged with long-chain lipid substrates. Therefore, the robust convergence between our empirical SDS-PAGE profile (resolving a prominent candidate band near 40 kDa) and the established proteomic baseline of the species strongly substantiates that the recovered biocatalytic stream is driven by an overexpressed candidate carboxylesterase domain native to *S. marcescens* 11E.

Based on these profiling checkpoints, the crude concentrate was subjected to preparative size-exclusion chromatography on a Sephadex G-100 matrix to achieve targeted functional fractionation. A total of 40 discrete fractions (2 mL each) were collected. Real-time absorbance tracking at 280 nm at the column exit was used successfully as an operational screening threshold to establish protein elution boundaries. The discrete distribution of the recovered esterase-like catalytic activity across the collected fractions is plotted in Figure 4.

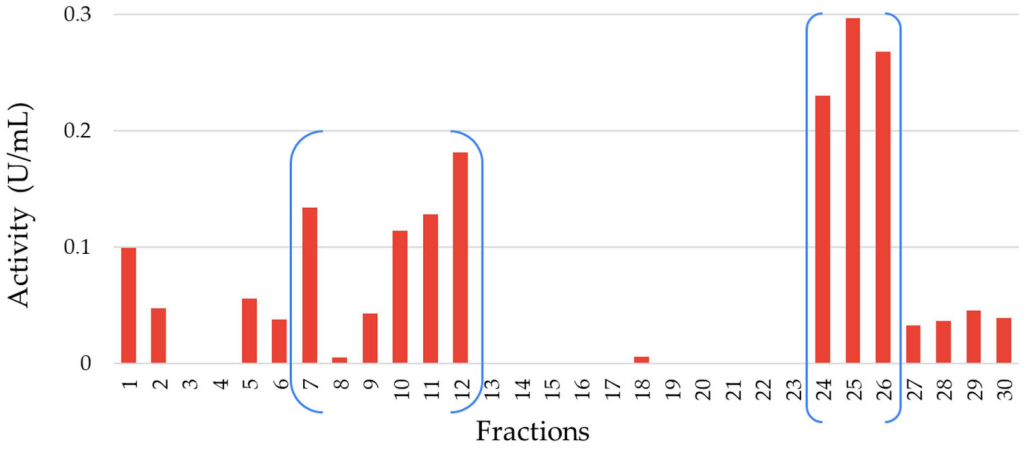

Figure 4. Preparative size-exclusion chromatography profiling of the concentrated extract on a Sephadex G-100 matrix. The plot illustrates the distribution of extracellular esterase-like catalytic activity (measured by pNPA hydrolysis) across 40 discrete fractions collected at a flow rate of 0.5 mL/min in 0.15 M Tris-HCl buffer (pH 8.5). The fractions enclosed in blue brackets indicate the successfully fractionated operational boundaries: Pool 1 (fractions 7–12) and Pool 2 (fractions 24–26).

The chromatographic run successfully resolved the activity into two independent, well-demarcated elution windows: Pool 1 (encompassing fractions 7–12) and Pool 2 (encompassing fractions 24–26). These active pools were independently harvested, concentrated via native ultrafiltration, and subjected to a comprehensive quantitative mass balance to evaluate downstream efficiency, as structurally consolidated in Table 3. Pool 1 and Pool 2 demonstrated specific activities of 17.8 ± 0.8 and 26.2 ± 1.2 U/mg against pNPA, respectively. Furthermore, to evaluate substrate affinity, both pools were tested against p-nitrophenyl butyrate (4C) and p-nitrophenyl octanoate (8C). The results confirmed a consistent preference for short-chain substrates in both fractions (Figure 5).

Table 3. Streamlined downstream purification and mass balance parameters for the extracellular esterase-like streams recovered from *Serratia marcescens* 11E.

Fractions	Total Protein (mg)	Total Activity (U)	Specific Activity (U/mg)	Recovery (%)	Purification Fold
Crude extract	3.94	64.45	16.36	100	1
Fractions 24–26	0.59	40.88	26.21	68.8	4.6
Fractions 7–12	0.85	23.57	17.8	67.3	3.1

Specific activities, recovery percentages, and purification folds were determined experimentally for each pooled fraction after concentration and standardization to a final volume of 10 mL. Total activity values reflect the measured activity of each pool. Therefore, these parameters should not be interpreted as additive in a conventional purification mass balance.

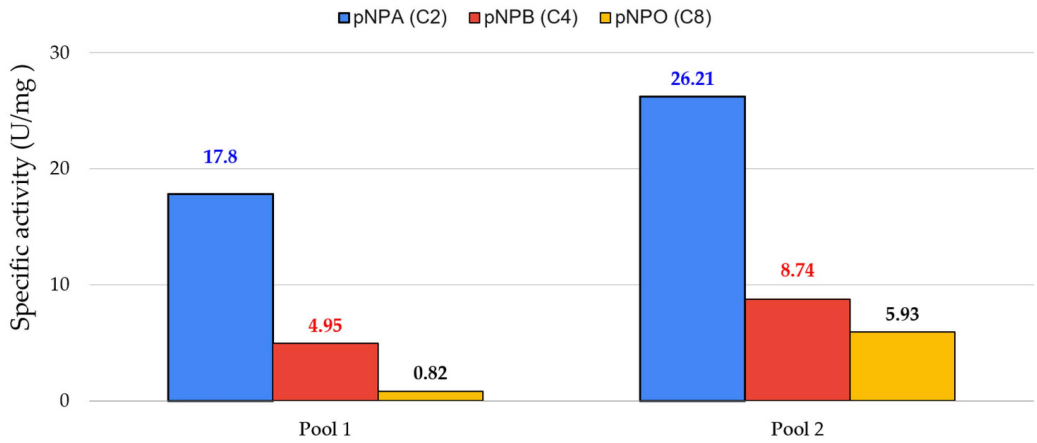

Figure 5. Specific activity (U/mg) of the recovered Pool 1 (fractions 7–12) and Pool 2 (fractions 24–26), evaluated across a panel of short- to medium-chain substrates: pNPA (p-nitrophenyl acetate, C2); pNPB (p-nitrophenyl butyrate, C4); and pNPO (p-nitrophenyl octanoate, C8).

4. Discussion

The qualitative screening on tributyrin agar supplemented with Tween 80 validated the baseline extracellular hydrolytic capacity of *Serratia marcescens* 11E when cultivated on the proposed co-valorization matrix. The development of a distinct precipitation halo firmly established the functional secretome profile of the wild-type strain, thereby justifying its selection for targeted bioprocess monitoring. Interestingly, the narrow diameter of the hydrolysis boundaries (<2 mm) has historically been associated with a predominantly carboxylesterase-like bias rather than a highly diffuse, true lipase footprint. Biochemically, carboxylesterases preferentially cleave water-soluble short-chain fatty acid esters (<8 carbons), whereas classical lipases display high turnover rates toward long-chain emulsified lipid domains through specialized interfacial activation mechanisms [39].

This enzymatic profile was effectively supported by the structural architecture of the 80:20 (*w*/*w*) vegetable wax and cheese whey matrix, which offered a complementary, dual-phase nutrient and physical environment during solid-state fermentation. On one hand, the aqueous cheese whey phase served as an immediate liquid vehicle, delivering highly bioavailable lactose, mineral salts, and trace proteins necessary for early biomass proliferation. On the other hand, the solid industrial vegetable wax residue provided the hydrophobic structural skeleton characteristic of supported SSF, while simultaneously supplying complex, long-chain saturated fatty acids. These lipid components can act as structural target triggers to stimulate the expression of baseline microbial hydrolases [40]. This synergistic multi-substrate design aligns with historical reports showing that wild-type *Serratia* species exhibit adaptive metabolic plasticity when exposed to lipid-rich residues (oils, waxes, and industrial fat co-products), especially under the localized, low-water-activity conditions that characterize high-yield SSF environments [41,42].

Following downstream recovery, the detailed substrate profiling of the cell-free concentrate confirmed that *S. marcescens* 11E selectively synthesizes an enzyme stream with a strong preference for short-chain esters over conventional, interface-dependent lipases. As expected, the catalytic specificity peaked sharply against p-nitrophenyl acetate (C2) and underwent a severe, chain-length-dependent decrease as the acyl structure expanded toward p-nitrophenyl butyrate (C4), octanoate (C8), and palmitate (C16) [43]. This marked preference for short-chain substrates represents a defining functional hallmark of classical carboxylesterases belonging to the α/β-hydrolase fold family [44]. Unlike lipases, these proteins typically possess a highly solvent-accessible catalytic triad that does not require a hydrophobic amphipathic alpha-helical "lid" to undergo interfacial opening [45]. Simi-

lar restrictive specificity hierarchies have been structurally documented for *S. marcescens* esterases such as EstA and EstB, which exhibit high specific activities toward C2–C4 esters while displaying negligible or baseline activity when challenged with long-chain C16 substrates [46]. Consequently, the catalytic trends captured in this study closely match the established biochemical consensus for the genus *Serratia*.

Regarding environmental variables, the crude extract exhibited a characteristically alkaline activity, with optimal performance initially resolved at 30 °C and pH 9.0. Extracellular hydrolases derived from *S. marcescens* and related *Enterobacteriaceae* frequently display evolutionarily conserved adaptations to alkaline environments, maintaining robust structural stability between pH 8.5 and 9.5, alongside operational thermal windows between 35 and 45 °C [34,39,42]. However, a particularly compelling feature of this extract was the detection of a distinct secondary activity peak at 70 °C under pH 9.0 conditions. Rather than prematurely asserting the presence of a genetic isoform, this interesting bimodal profile can be critically cross-referenced with our size-exclusion chromatography data. The resolution of the active extract into two distinct elution windows (Pool 1 and Pool 2) strongly indicates that the candidate carboxylesterase coexists in multiple structural assembly forms or distinct quaternary aggregation states, each with specific thermal stabilities and localized variations in active-site accessibility under thermal stress. Although size-exclusion chromatography data provided evidence of bimodal activity, further studies could be carried out for confirmation, such as cellular fractionation [47].

Additionally, complementary microenvironmental dynamics cannot be ruled out, as residual low-molecular-weight components in the industrial vegetable wax matrix might act as non-denaturing hydrophobic stabilizers or as natural surfactant-like scaffolds. In this context, wild-type *S. marcescens* strains are well-documented producers of extracellular lipopeptide biosurfactants, such as serrawattins, particularly when cultivated on lipid-dense substrates [48]. The co-presence of these endogenous tensoactive molecules in crude extracts can provide a protective micellar microenvironment, effectively preserving the structural integrity and catalytic activity of extracellular hydrolases under severe thermal stress [39]. This physical and functional resilience at elevated temperatures warrants deeper structural investigation in future execution phases, as it provides a valuable operational advantage for translating these streams into harsh industrial bioprocess settings.

To further track downstream protein clearance and monitor these structural candidate fractions, SDS-PAGE proved crucial. The resolving gel revealed a single prominent monomeric band migrating at approximately 40 kDa. Crucially, the successful concentration of this enzyme stream using a 50-kDa MWCO membrane under native conditions strongly supports the hypothesis that, in its active, non-denatured state, the protein may form oligomeric structures or stable macromolecular complexes with residual components of the vegetable wax matrix, thereby increasing its effective hydrodynamic volume during filtration. Nevertheless, under denaturing conditions, the resolution of this well-defined 40 kDa band aligns precisely with the documented monomeric molecular masses of wild-type *S. marcescens* carboxylesterases, which typically range from 38 to 42 kDa [37,38,40,41]. In contrast, extracellular lipases from this genus, such as the classical LipA, exhibit higher molecular masses (45–65 kDa) and are structurally characterized by broader, interface-dependent catalytic profiles that efficiently act on long-chain triglycerides [37].

The subsequent preparative size-exclusion chromatography on Sephadex G-100 successfully achieved targeted functional fractionation, yielding two distinct active streams (Pool 1 and Pool 2) with purification enrichments of 3.1 and 4.6-fold, respectively, in specific activity toward short-chain substrates. This operational concentration is highly noteworthy, as extracellular enzymes derived from SSF are notoriously difficult to fractionate due to the complex, heterogeneous nature of agro-industrial matrices, which often co-elute with

interfering pigments, humic-like substances, and sticky polyphenolic complexes [49]. By bypassing high-salt ion-exchange steps that would trigger extensive mass-transfer losses and require additional desalting cycles, this streamlined preparative configuration successfully preserved the catalytic mass balance of the small-scale SSF batch. Overall, this exploratory study successfully demonstrates the baseline feasibility of co-valorizing carbohydrate-rich dairy effluents and lipid-rich industrial wax wastes into functionally resilient, candidate esterase-like protein streams. This dual-benefit approach establishes a foundational proof-of-concept that directly aligns with contemporary principles of the circular bioeconomy and sustainable downstream processing in the industrial biotechnology sector.

5. Conclusions and Perspectives

This exploratory study successfully establishes the baseline feasibility of using a novel, supported solid-state fermentation (SSF) matrix composed of cheese whey and vegetable wax residues to produce extracellular streams exhibiting robust esterase-like activity by *Serratia marcescens* 11E. The strategic development of this 80:20 (*w*/*w*) co-valorization framework demonstrates that low-cost, nutrient-rich industrial by-products can be synergistically repurposed as sustainable, high-yielding fermentation matrices without requiring complex multi-variable optimization.

Biochemically, the recovered cell-free extract displays a distinct functional profile characteristic of microbial carboxylesterases, exhibiting a strict catalytic preference for short-chain substrates (pNPA > pNPB) over long-chain fatty acid esters (pNPP). The extract exhibits alkaline-active behavior, with optimal performance initially at 30 °C and pH 9, along with a resilient, bimodal catalytic peak resolved at 70 °C. While denaturing electrophoresis (SDS-PAGE) resolved a prominent candidate protein band migrating at approximately 40 kDa, consistent with esterases from *S. marcescens*, definitive assignment of molecular identity and family classification remains at the operational hypothesis stage.

To expand the boundaries of this foundational proof-of-concept, future perspectives will focus on deploying high-resolution validation milestones. Ongoing research is directed toward performing zymography, precise proteomic sequencing, and comparative genomic characterization to structurally confirm the identity of the active enzyme and elucidate the mechanisms underlying the high-temperature bimodal resilience. Additionally, subsequent engineering phases will include optimizing reactor-scale SSF architectures, developing matrix immobilization protocols to enhance biocatalytic reusability, and operational evaluation of these resilient candidate streams in targeted food processing and industrial biotechnology settings.

Supplementary Materials: The following supporting information can be downloaded at: https://www.mdpi.com/article/10.3390/pr14132089/s1, Figure S1: Appearance of *Serratia marcescens* 11E inoculated on LB agar after 24 h of incubation (left) and Gram-stain (right).

Author Contributions: Conceptualization, F.J.A.-V., M.M.R.-D. and J.F.V.-C.; methodology, F.J.A.-V., I.C.A.-D.L. and E.A.B.-G.; formal analysis, G.E.Q.-V., E.A.B.-G. and I.C.A.-D.L.; investigation, F.J.A.-V., J.F.V.-C. and M.M.R.-D.; writing—original draft preparation, F.J.A.-V., I.C.A.-D.L., E.A.B.-G. and J.F.V.-C.; writing—review and editing, J.F.V.-C. and M.M.R.-D. All authors have read and agreed to the published version of the manuscript.

Funding: This research received no external funding.

Data Availability Statement: The original contributions presented in this study are included in the article. Further inquiries can be directed to the corresponding authors.

Acknowledgments: The authors would like to thank the Secretaría de Ciencia, Humanidades, Tecnología e Innovación (SECIHTI) for the scholarships provided to Francisco Javier Aranda Valdes

("Becas Nacionales" 1334212) and Gabriela Elizabeth Quintanilla-Villanueva ("Estancias Postdoctorales por México" 740156).

Conflicts of Interest: The authors declare no conflicts of interest.

References

1. UN Environment Programme. Global Waste Management Outlook 2024 | UNEP—UN UN Environment Programme. Available online: https://www.unep.org/resources/global-waste-management-outlook-2024 (accessed on 25 February 2024).
2. Yafetto, L. Application of solid-state fermentation by microbial biotechnology for bioprocessing of agro-industrial wastes from 1970 to 2020: A review and bibliometric analysis. *Heliyon* **2022**, *8*, e09173. [CrossRef] [PubMed]
3. López-Gómez, J.P.; Manan, M.A.; Webb, C. Chapter 7—Solid-state fermentation of food industry wastes. In *Food Industry Wastes*, 2nd ed.; Kosseva, M.R., Webb, C., Eds.; Academic Press: San Diego, CA, USA, 2020; pp. 135–161. [CrossRef]
4. Bulgari, D.; Renzetti, S.; Messgo-Moumene, S.; Monti, E.; Gobbi, E. Optimization of Esterase Production in Solid-State Fermentation of Agricultural Digestate. *Fermentation* **2023**, *9*, 524. [CrossRef]
5. Uraji, M.; Arima, J.; Inoue, Y.; Harazono, K.; Hatanaka, T. Application of two newly identified and characterized feruloyl esterases from *Streptomyces* sp. In the enzymatic production of ferulic acid from agricultural biomass. *PLoS ONE* **2014**, *9*, e104584. [CrossRef] [PubMed]
6. Rodriguez-Couto, S.; Sanromán, M. Application of Solid-State Fermentation to Food Industry—A Review. *J. Food Eng.* **2006**, *76*, 291–302. [CrossRef]
7. Foo, W.H.; Chia, W.Y.; Tang, D.Y.Y.; Koay, S.S.N.; Lim, S.S.; Chew, K.W. The conundrum of waste cooking oil: Transforming hazard into energy. *J. Hazard. Mater.* **2021**, *417*, 126129. [CrossRef] [PubMed]
8. Cheng, D.; Liu, Y.; Ngo, H.H.; Guo, W.; Chang, S.W.; Nguyen, D.D.; Zhang, S.; Luo, G.; Bui, X.T. Sustainable enzymatic technologies in waste animal fat and protein management. *J. Environ. Manag.* **2021**, *284*, 112040. [CrossRef] [PubMed]
9. Mou, J.-H.; Yan, W.; Qin, Z.-H.; Haque, M.A.; Miao, Y.-H.; Xin, F.-X.; Wang, X.; Fickers, P.; Lin, C.S.K. Food waste from various origins as feedstocks for recombinant protein production by *Yarrowia lipolytica* using in situ fibrous bed bioreactor. *Chem. Eng. J.* **2024**, *481*, 148408. [CrossRef]
10. Sánchez, A.; Oiza, N.; Artola, A.; Font, X.; Barrena, R.; Moral-Vico, J.; Gea, T. Solid-state fermentation: A review of its opportunities and challenges in the framework of circular bioeconomy. *Afinidad J. Chem. Eng. Theor. Appl. Chem.* **2024**, *81*, 51–57. [CrossRef] [PubMed]
11. Ali, S.; Khan, S.A.; Hamayun, M.; Lee, I.-J. The Recent Advances in the Utility of Microbial Lipases: A Review. *Microorganisms* **2023**, *11*, 510. [CrossRef] [PubMed]
12. Raveendran, S.; Parameswaran, B.; Ummalyma, S.B.; Abraham, A.; Mathew, A.K.; Madhavan, A.; Rebello, S.; Pandey, A. Applications of microbial enzymes in food industry. *Food Technol. Biotechnol.* **2018**, *56*, 16. [CrossRef] [PubMed]
13. Guerrand, D. Lipases industrial applications: Focus on food and agroindustries. *OCL Oilseeds Fats Crops Lipids* **2017**, *24*, D403. [CrossRef]
14. Aravindan, R.; Anbumathi, P.; Viruthagiri, T. Lipase applications in food industry. *Indian J. Biotechnol.* **2007**, *6*, 141.
15. Panda, T.; Gowrishankar, B.S. Production and applications of esterases. *Appl. Microbiol. Biotechnol.* **2005**, *67*, 160–169. [CrossRef] [PubMed]
16. Mattedi, A.; Sabbi, E.; Farda, B.; Djebaili, R.; Mitra, D.; Ercole, C.; Cacchio, P.; Del Gallo, M.; Pellegrini, M. Solid-State Fermentation: Applications and Future Perspectives for Biostimulant and Biopesticides Production. *Microorganisms* **2023**, *11*, 1408. [CrossRef] [PubMed]
17. Gupta, B.; Gupta, K.; Mukherjee, S. Lipase production by Serratia marcescens strain SN5gR isolated from the scat of lion-tailed macaque (*Macaca silenus*) in Silent Valley National Park, a biodiversity hotspot in India. *Ann. Microbiol.* **2013**, *63*, 649–659. [CrossRef]
18. Long, Z.-D.; Xu, J.-H.; Pan, J. Significant Improvement of Serratia marcescens Lipase Fermentation, by Optimizing Medium, Induction, and Oxygen Supply. *Appl. Biochem. Biotechnol.* **2007**, *142*, 148–157. [CrossRef] [PubMed]
19. Fibriana, F.; Upaichit, A.; Cheirsilp, B. Turning waste into valuable products: Utilization of agroindustrial oily wastes as the low-cost media for microbial lipase production. *J. Phys. Conf. Ser.* **2021**, *1918*, 052028. [CrossRef]
20. Joseph, B.; Upadhyaya, S.; Ramteke, P. Production of Cold-Active Bacterial Lipases through Semisolid State Fermentation Using Oil Cakes. *Enzym. Res.* **2011**, *2011*, 796407. [CrossRef] [PubMed]
21. Hölker, U.; Höfer, M.; Lenz, J. Biotechnological advantages of laboratory-scale solid-state fermentation with fungi. *Appl. Microbiol. Biotechnol.* **2004**, *64*, 175–186. [CrossRef] [PubMed]
22. Oiza, N.; Moral-Vico, J.; Sánchez, A.; Oviedo, E.R.; Gea, T. Solid-State Fermentation from Organic Wastes: A New Generation of Bioproducts. *Processes* **2022**, *10*, 2675. [CrossRef]

23. Faisal, P.A.; Hareesh, E.S.; Priji, P.; Unni, K.N.; Sajith, S.; Sreedevi, S.; Josh, M.S.; Benjamin, S. Optimization of parameters for the production of lipase from *Pseudomonas* sp. BUP6 by solid state fermentation. *Adv. Enzym. Res.* **2014**, *2*, 125.
24. Santis-Navarro, A.; Gea, T.; Barrena, R.; Sánchez, A. Production of lipases by solid state fermentation using vegetable oil-refining wastes. *Bioresour. Technol.* **2011**, *102*, 10080–10084. [CrossRef] [PubMed]
25. Sahoo, R.K.; Kumar, M.; Mohanty, S.; Sawyer, M.; Rahman, P.K.; Sukla, L.B.; Subudhi, E. Statistical optimization for lipase production from solid waste of vegetable oil industry. *Prep. Biochem. Biotechnol.* **2018**, *48*, 321–326. [CrossRef] [PubMed]
26. Claes, A.; Deparis, Q.; Foulquié-Moreno, M.R.; Thevelein, J.M. Simultaneous secretion of seven lignocellulolytic enzymes by an industrial second-generation yeast strain enables efficient ethanol production from multiple polymeric substrates. *Metab. Eng.* **2020**, *59*, 131–141. [CrossRef]
27. Hess, M. Thermoacidophilic proteins for biofuel production. *Trends Microbiol.* **2008**, *16*, 414–419. [CrossRef]
28. Diez, M.C.; Llafquen, C.; Fincheira, P.; Lamilla, C.; Briceño, G.; Schalchli, H. Biosurfactant Production by *Bacillus amyloliquefaciens* C11 and *Streptomyces lavendulae* C27 Isolated from a Biopurification System for Environmental Applications. *Microorganisms* **2022**, *10*, 1892. [CrossRef]
29. Moya-Ramírez, I.; Tsaousi, K.; Rudden, M.; Marchant, R.; Jurado-Alameda, E.; García-Román, M.; Banat, I.M. Rhamnolipid and surfactin production from olive oil mill waste as sole carbon source. *Bioresour. Technol.* **2015**, *198*, 231–236. [CrossRef]
30. Hernandez-Velasco, P.; Morales-Atilano, I.; Rodríguez-Delgado, M.; Rodríguez-Delgado, J.M.; Luna-Moreno, D.; Ávalos-Alanís, F.G.; Villarreal-Chiu, J.F. Photoelectric evaluation of dye-sensitized solar cells based on prodigiosin pigment derived from Serratia marcescens 11E. *Dye. Pigment.* **2020**, *177*, 108278. [CrossRef]
31. AOAC INTERNATIONAL. Official Methods of Analysis of the AOAC 969.33. In *Fatty Acids in Oils and Fats*; AOAC: Arlington, VA, USA, 2000.
32. Secretaría de Salud (SSA). *NOM-116-SSA1-1994: Determination of Moisture in Foods by Heat Treatment. Sand or Gauze Method*; Ministry of Health: Mexico City, Mexico, 1994. Available online: https://www.dof.gob.mx/nota_to_imagen_fs.php?codnota=4879241&fecha=10/08/1995&cod_diario=209265 (accessed on 26 April 2025).
33. Secretaría de Salud (SSA). *NOM-086-SSA1-1994: Food and Non-Alcoholic Beverages with Modifications to Their Composition. Nutritional Specifications*; Ministry of Health: Mexico City, Mexico, 1994. Available online: https://www.dof.gob.mx/nota_to_imagen_fs.php?codnota=4890075&fecha=26/06/1996&cod_diario=209540 (accessed on 26 April 2025).
34. Juntachai, W.; Kajiwara, S. Differential Expression of Extracellular Lipase and Protease Activities of Mycelial and Yeast Forms in Malassezia furfur. *Mycopathologia* **2015**, *180*, 143–151. [CrossRef] [PubMed]
35. Bradford, M.M. A rapid and sensitive method for the quantitation of microgram quantities of protein utilizing the principle of protein-dye binding. *Anal. Biochem.* **1976**, *72*, 248–254. [CrossRef] [PubMed]
36. Laemmli, U.K. Cleavage of Structural Proteins during the Assembly of the Head of Bacteriophage T4. *Nature* **1970**, *227*, 680–685. [CrossRef] [PubMed]
37. Jiang, H.; Zhang, S.; Gao, H.; Hu, N. Characterization of a cold-active esterase from *Serratia* sp. And improvement of thermostability by directed evolution. *BMC Biotechnol.* **2016**, *16*, 7. [CrossRef] [PubMed]
38. Bhardwaj, K.K.; Kishen, S.; Mehta, A.; Sharma, A.; Gupta, R. Purification of high molecular weight thermotolerant esterase from *Serratia* sp. And its characterization. *3 Biotech* **2021**, *11*, 308. [CrossRef] [PubMed]
39. Chandra, P.; Enespa Singh, R.; Arora, P.K. Microbial lipases and their industrial applications: A comprehensive review. *Microb. Cell Factories* **2020**, *19*, 169. [CrossRef] [PubMed] [PubMed Central]
40. Adlan, N.A.; Sabri, S.; Masomian, M.; Ali, M.S.M.; Rahman, R.N.Z.R.A. Microbial Biodegradation of Paraffin Wax in Malaysian Crude Oil Mediated by Degradative Enzymes. *Front. Microbiol.* **2020**, *11*, 565608. [CrossRef] [PubMed]
41. Henriette, C.; Zinebi, S.; Aumaitre, M.F.; Petitdemange, E.; Petitdemange, H. Protease and lipase production by a strain of Serratia marcescens (532 S). *J. Ind. Microbiol.* **1993**, *12*, 129–135. [CrossRef]
42. Nascimento, F.V.; do Lemes, A.C.; Castro, A.M.; de Secchi, A.R.; Zarur Coelho, M.A. A Temporal Evolution Perspective of Lipase Production by *Yarrowia lipolytica* in Solid-State Fermentation. *Processes* **2022**, *10*, 381. [CrossRef]
43. Fojan, P.; Jonson, P.H.; Petersen, M.T.N.; Petersen, S.B. What distinguishes an esterase from a lipase: A novel structural approach. *Biochimie* **2000**, *82*, 1033–1041. [CrossRef] [PubMed]
44. Riedel, K.; Talker-Huiber, D.; Givskov, M.; Schwab, H.; Eberl, L. Identification and characterization of a GDSL esterase gene located proximal to the swr quorum-sensing system of Serratia liquefaciens MG1. *Appl. Environ. Microbiol.* **2003**, *69*, 3901–3910. [CrossRef] [PubMed]
45. Akatsuka, H.; Kawai, E.; Sakurai, N.; Omori, K. The *Serratia marcescens bioH* gene encodes an esterase. *Gene* **2003**, *302*, 185–192. [CrossRef] [PubMed]
46. Akatsuka, H.; Kawai, E.; Omori, K.; Komatsubara, S.; Shibatani, T.; Tosa, T. The lipA gene of Serratia marcescens which encodes an extracellular lipase having no N-terminal signal peptide. *J. Bacteriol.* **1994**, *176*, 1949–1956. [CrossRef] [PubMed]
47. Aridor-Piterman, O.; Lavie, Y.; Liscovitch, M. Bimodal distribution of phosphatidic acid phosphohydrolase in NG108–15 cells: Modulation by the amphiphilic lipids oleic acid and sphingosine. *Eur. J. Biochem.* **1992**, *204*, 561–568. [CrossRef]

48. Chen, W.C.; Kan, K.H.; Wang, L.F.; Wei, Y.H. Characterization and production of serrawettin, a lipopeptide biosurfactant, from *Serratia marcescens* SMΔR. *J. Taiwan Inst. Chem. Eng.* **2024**, *160*, 105232. [CrossRef]
49. Lizardi-Jiménez, M.A.; Hernández-Martínez, R. Solid state fermentation (SSF): Diversity of applications to valorize waste and biomass. *3 Biotech* **2017**, *7*, 44. [CrossRef] [PubMed] [PubMed Central]